Electronic supplementary information (ESI):

Dealloying induced plasmonic Au nanoparticles modified mesoporous TiO_2 for enhanced visible light photocatalysis

Zhengfeng Zhao, Xiaoxia Zhu, Min Zuo, Jing Xu and Yan Wang*

School of Materials Science & Engineering, University of Jinan, No. 336, West Road of Nan Xinzhuang, Jinan 250022, PR China

* Corresponding author. Tel: +86-531-82765473; Fax: +86-531-87974453

E-mail address: mse_wangy@ujn.edu.cn (Yan Wang).

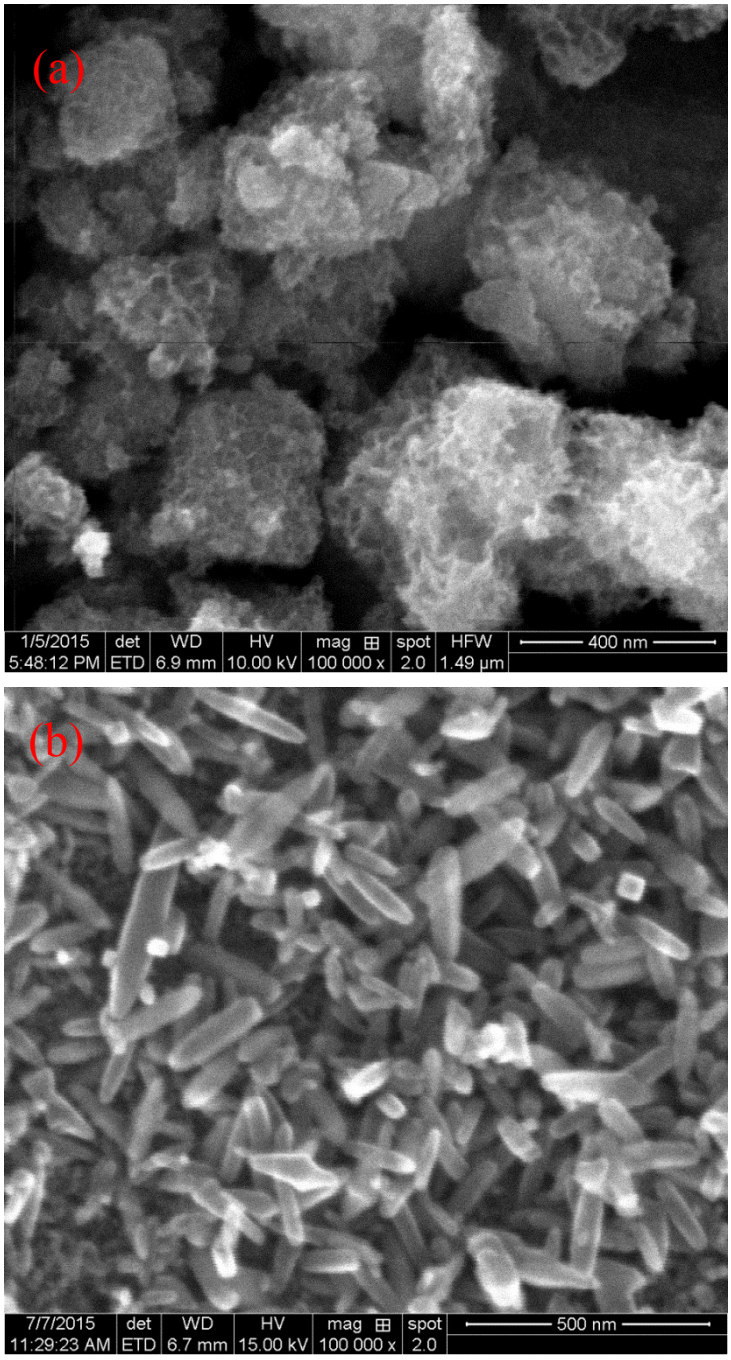

Fig. S1 The SEM images of the (a) TiO_2-C and (b) TiO_2-H.

The pure TiO_2 was fabricated using the Al-Ti precursor alloy. The TiO_2-C obtained by the calcination of the H-titanate presents the 3D network structure (Fig. S1(a)). Fig. S1(b) shows the spindle-like anatase TiO_2 obtained by hydrothermal treatment of H-titanate.

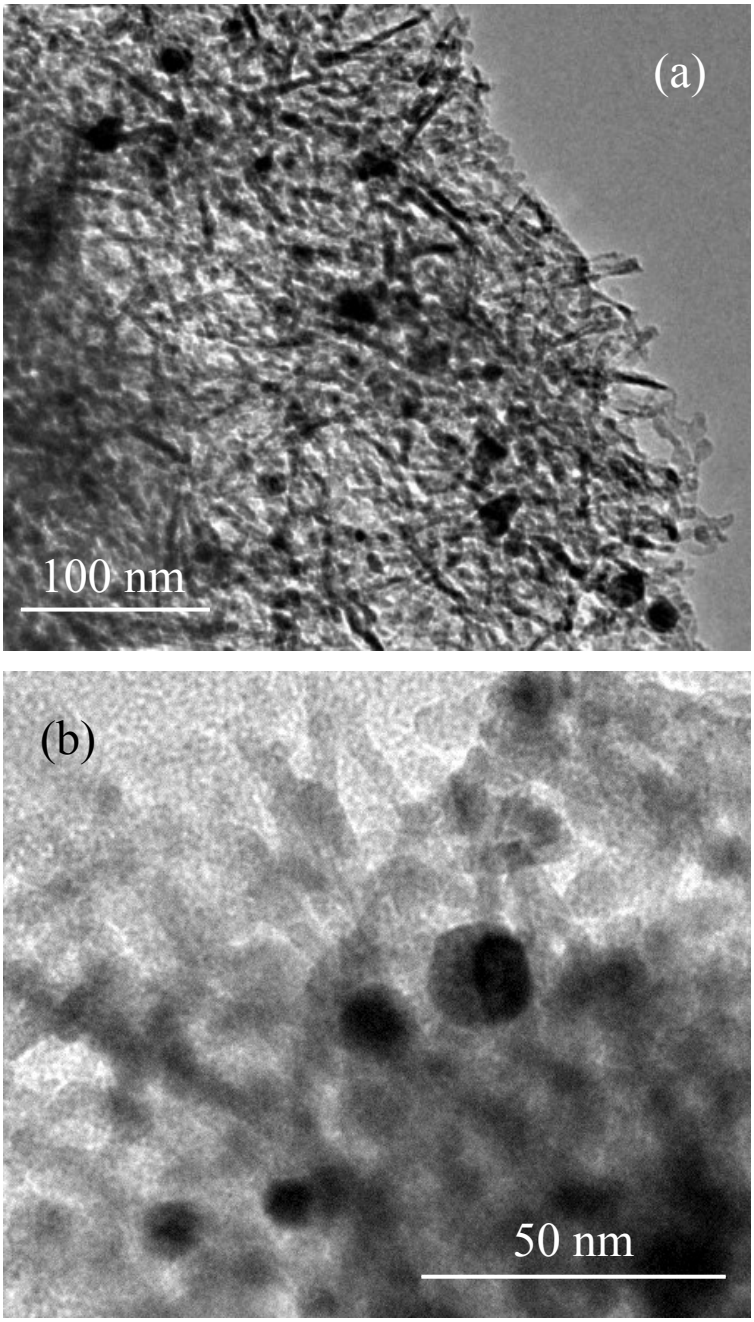

Fig. S2 The TEM images of the Au/TiO_2-C photocatalyst.

Fig. S2 shows that the Au nanoparticles are embedded in the 3D network structure of anatase TiO_2 matrix.

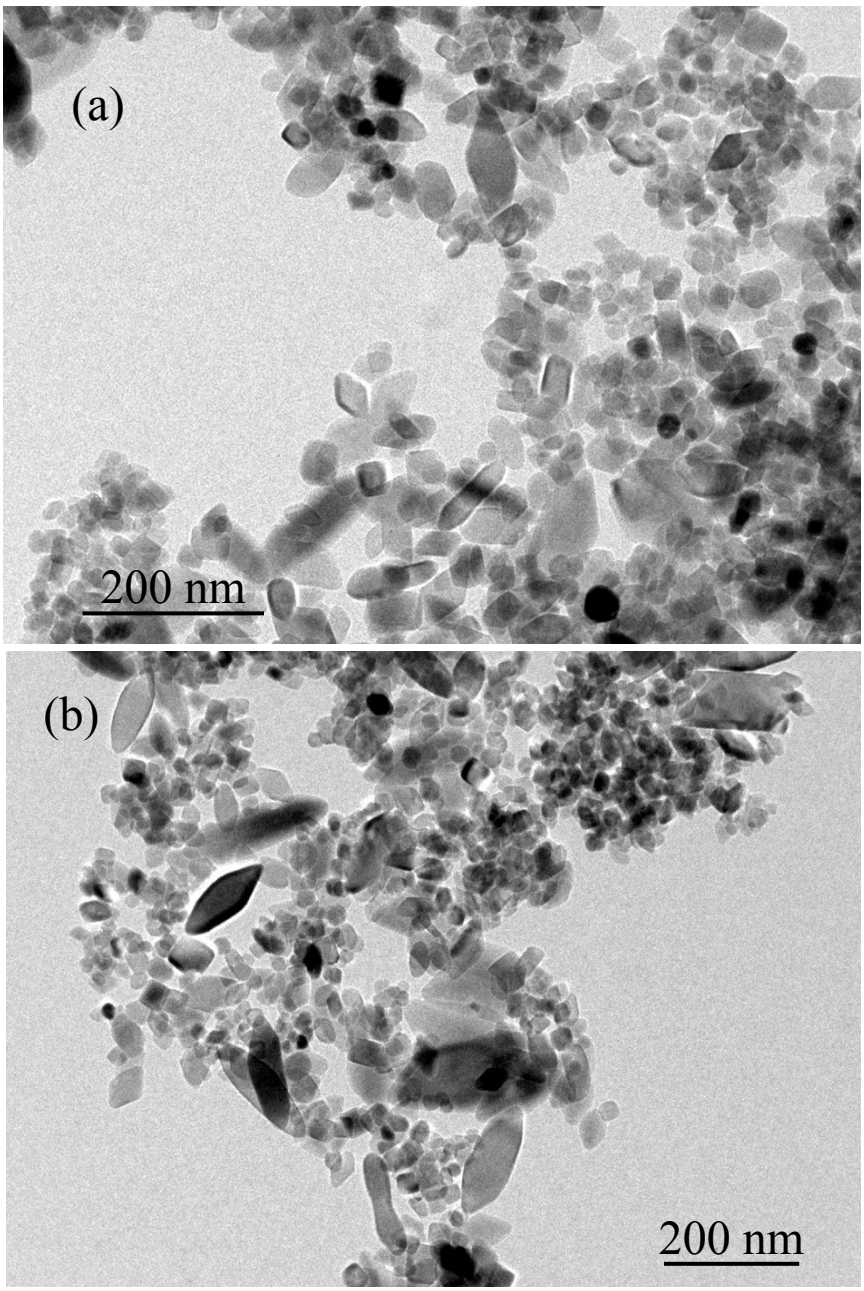

Fig. S3 The TEM images of the Au/TiO_2-H photocatalyst.

Fig. S3 shows the uneven distribution of Au nanoparticles (the black spots). The regular shaped TiO_2 and the Au nanoparticles are separated from each other.

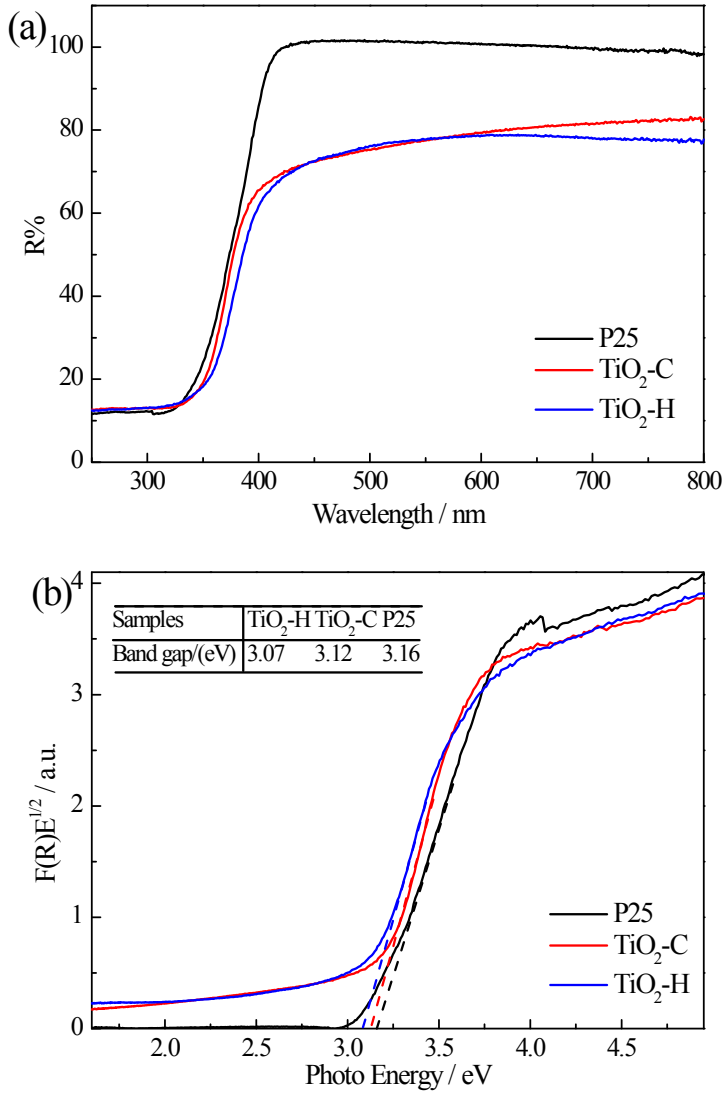

Fig. S4 (a)UV-Vis diffuse reflectance spectra (DRS) of different photocatalysts, (b) plots transformed according to the Kubelka-Munk function versus energy of light for the photocatalysts.

Fig. S4(a) shows the DRS of the pure TiO_2. The TiO_2-C and TiO_2-H samples present the absorption for visible light by comparing with the commercial P25. Fig. S4(b) shows the plots of $(F(R)E)^{1/2}$ versus the energy of absorbed light. Obviously, the TiO_2-C and TiO_2-H present the narrower band gap than P25. These results may result from the multiple reflection of light in the mesopores which extends in the path way of light.

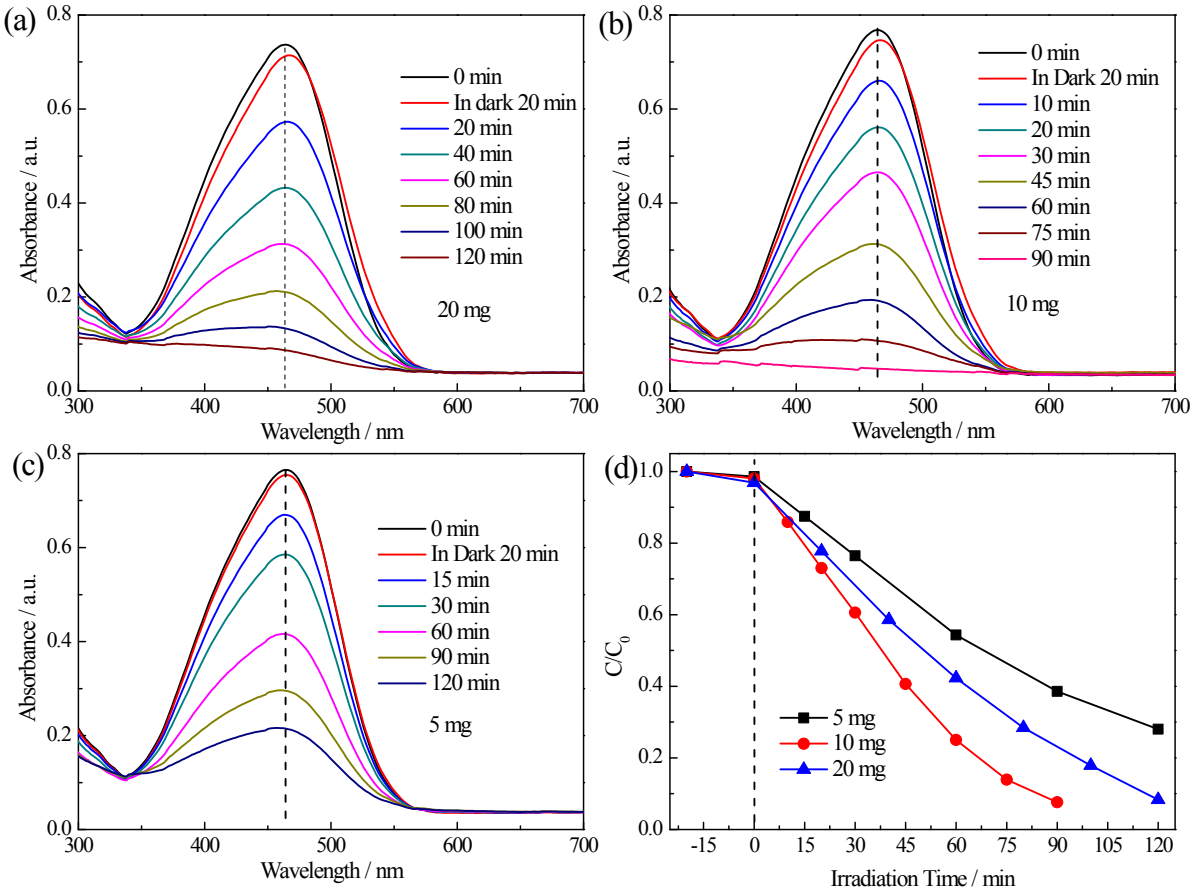

Fig. S5 (a-c) UV-vis absorption spectra of MO solution under different irradiation time in the presence of Au/TiO_2-C with different dosages. (d) Comparison of photocatalytic efficiencies of Au/TiO_2-C with different dosages.

The photocatalyst can shade part of the light, which reduces the photocatalytic efficiency. In order to obtain the optimum photocatalytic efficiency, the different dosages of the Au/TiO_2-C were used to photodegrade the MO solution. Fig. S5(a-c) show the UV-vis absorption spectra of MO solutions during the photocatalysis by different dosages of the Au/TiO_2-C. Fig. S5(d) presents the comparison of photocatalytic efficiencies. When the dosage of Au/TiO_2-C is 10 mg, the fastest degradation rate is reached.

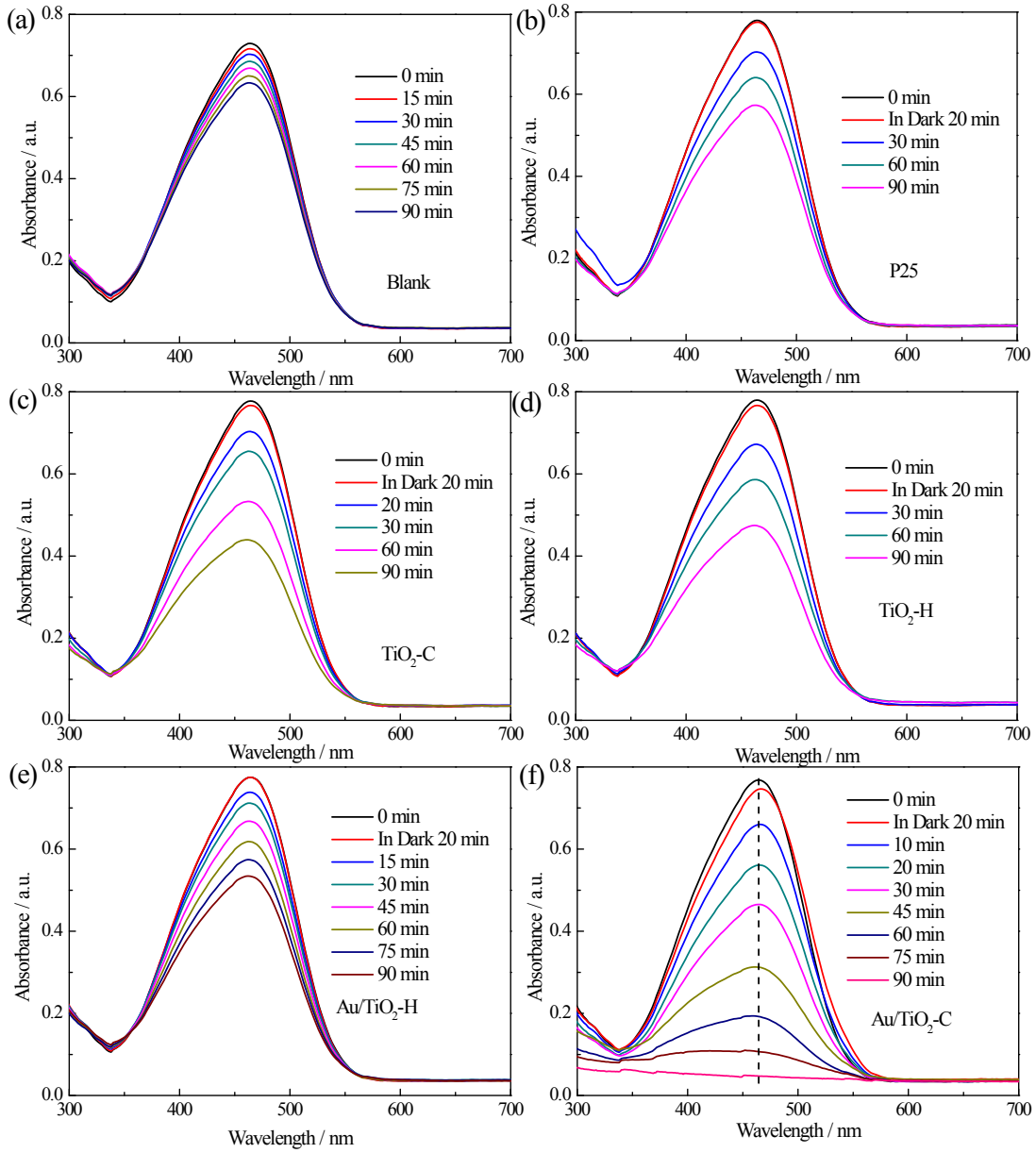

Fig. S6 UV-vis absorption spectra of MO solution under different irradiation time in the presence of different photocatalysts with10 mg. (a) Blank, (b) P25, (c) TiO_2-C, (d) TiO_2-H, (e) Au/TiO_2-H and (f) Au/TiO_2-C.

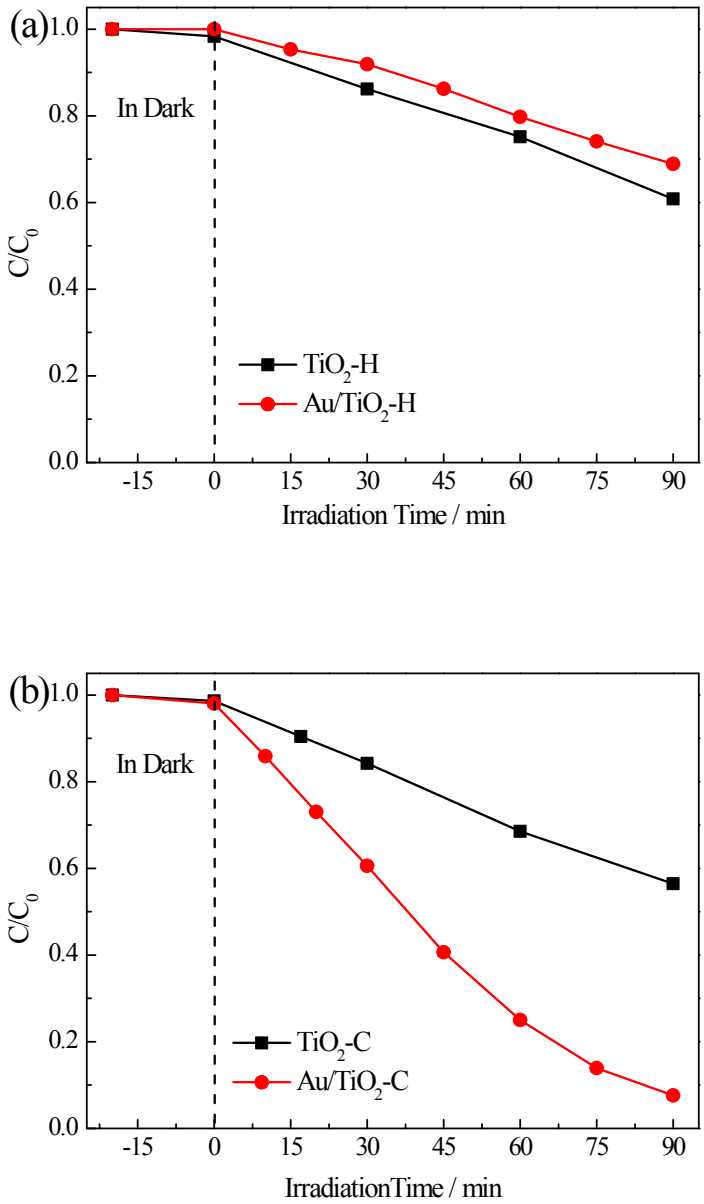

Fig. S7 Comparison of photocatalytic efficiencies between pure TiO_2 and Au/TiO_2 composites. The photocatalysts were fabricated by the (a) hydrothermal and (b) calcination methods.

Fig. S7(a) shows the photocatalytic efficiencies of TiO_2-H and Au/TiO_2-H samples. Obviously, the induced Au nanoparticles do not improve the photocatalytic activity. However, the Au/TiO_2-C shows the enhanced photocatalytic activity by comparing with the TiO_2-C (Fig. S7(b)). Of importance, the two kinds of pure TiO_2

with different specific surface area show the similar photocatalytic activities (the photodegradation efficiencies are about 40%). It means that the specific surface area is not a decisive factor for the photocatalytic activities.

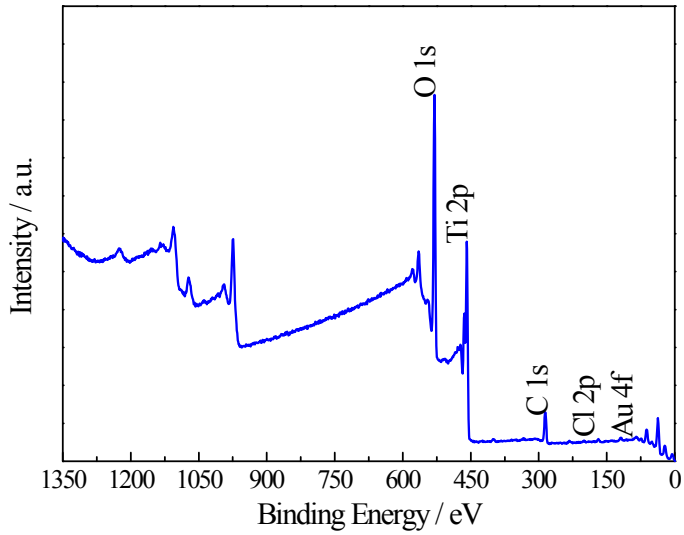

Fig. S8 XPS survey spectrum of the Au/TiO_2-C.